Biochimica et Biophysica Acta 862 (1986) 17–26
Elsevier

BBA 73313

Reversible changes in myelin structure and electrical activity during anesthesia in vivo

Leonardo Mateu and O. Morán *

Laboratorio de Estructura Molecular, Centro de Biofísica y Bioquímica, Instituto Venezolano de Investigaciones Científicas, IVIC, Apartado 21827, Caracas 1020-A (Venezuela)

(Received 17 April 1986)
(Revised manuscript received 28 July 1986)

Key words: Myelin structure; Anesthetic–membrane interaction; Stabilizing force; Action potential; X-ray diffraction

X-ray diffraction patterns have been recorded from sciatic nerve myelin by means of dynamic X-ray diffraction either from frogs, during the early stages of anesthesia in vivo induced by *n*-pentane inhalation, and from frog and rat sciatic nerves isolated immediately after the animal was anesthetized. This approach has enabled to resolve minor changes in myelin structure that occur during anesthesia which were found to be similar in frogs and mammals. The X-ray patterns show a reversible slight decrease in intensity of the even reflections during anesthesia. The electron density profiles from myelin of anesthetized and recovered nerves revealed that the unit membrane structure is practically identical in both circumstances. However, during anesthesia myelin membrane pairs move toward the cytoplasmic side becoming more closely packed by 1.6 Å. Physiological activity was estimated during the recovery process: compound action potential recovered its maximal amplitude before myelin recovered its native structure. On the contrary, the conduction velocity seemed to be closely related to the structural recovery. This work provides evidence that early stages of anesthesia by *n*-pentane in vivo does not change membrane bilayer structure but perturbs the surface interactions between adjacent membrane pairs.

Introduction

Although a wealth of information about the electrophysiological and membrane perturbating properties of various classes of anesthetics has been accumulated using a wide variety of experimental approaches, the molecular mechanisms by means of which these substances alter the functioning of excitable tissues is far from established. Most of the current theories of anesthesia are based on the assumption that anesthetics act on the hydrophobic regions of nerve cell membranes, attributing the effects to the number of molecules dissolved in the excitable plasma membrane (see Refs. 1 and 2 for a review). Most anesthetics have been shown to disorder lipid bilayers [3–7] and it is generally accepted that anesthetics increase the fluidity of cell membranes. However, it is still an open question whether these changes are critical in producing anesthesia. The observation that both these changes and anesthesia are reversed by pressure [6–10] has suggested that a net volume increase is involved in this phenomenon.

Other lines of thought stress changes induced by anesthetics on the properties of water molecules at the surface of proteins and biological

* Present address: Centro de Biociencias, Instituto Internacional de Estudios Avanzados (IDEA), Apartado 17606, Caracas 1015-A, Venezuela.
Correspondence: Dr. L. Mateu, Laboratorio de Estructura Molecular, Centro de Biofísica y Bioquímica, Instituto Venezolano de Investigaciones Científicas, IVIC, Apartado 21827, Caracas 1020-A, Venezuela.

membranes [11,12]. Thus, it has been proposed [13,14] that modification of the interfacial water structure and the net volume increase associated with the anesthetic effect may be relevant in perturbing the physiological properties of membranes. Newly formed salt bridges involving membrane proteins could be responsible of the changes in biological activities. These ideas are supported by experimental findings [15–17] which have evidenced specific ion effects in relation to water structure at interfaces in biological systems as a consequence of anesthetic treatments.

Our interest for anesthesia started few years ago after we got acquainted with the proposal that the anesthetic effect of *n*-alkanes is due to a thickening of the membrane lipid bilayer, which destabilizes the excitable ionic channels [18]. In order to verify this hypothesis it was decided to investigate the effect of *n*-alkanes on the structure of a membrane system such as the nerve myelin sheath, which has the advantages of being both, naturally ordered and involved in nerve conduction [19,20]. We performed an X-ray diffraction study testing the effect of the perfusion of isolated frog sciatic nerves with normal Ringer solutions saturated with *n*-alkanes, simultaneously we obtained data of myelin structure and nerve electrical activity [21,22]. The results indicated that the effect of *n*-alkanes is two-fold: (a) an initial reversible phase, characterized by a continuous intensity change of the 3rd and 4th order reflections of the X-ray diffraction patterns, which is concomitant with a fall in the compound action potential; (b) a final irreversible phase, consisting of an increase in the membrane bilayer thickness which occurs several hours after the complete elimination of the electrical activity. Unfortunately, the structural modifications occurring concomitantly with changes in physiological activity (initial phase) were not determined due to the limited resolution of the X-ray patterns from *n*-pentane-treated sciatic nerves [22]. Thus, to resolve the changes in myelin structure which occurred simultaneously with the process of anesthesia, accurate X-ray diagrams at the highest possible resolution had to be recorded in very short times. In consequence we have improved the original set-up [22]. Now, experiments of general anesthesia in a whole animal can be performed and the anesthetic effects on peripheral myelin can be studied at the molecular level. We have observed minor but significant changes in the X-ray reflections and in electrical parameters (compound action potential and conduction velocity) of sciatic nerves from frogs and rats anesthetized in vivo by inhalation of *n*-pentane vapors. The structural changes are reversible and consist of a movement of the myelin membrane pairs towards the cytoplasmic side.

Methods

Nerves. Intact sciatic nerves were studied from frogs (*Rana pipiens* and rats (*Ratus norvegicus*), either in vivo or isolated after the animals were previously anesthetized by breathing *n*-pentane vapors.

Experimental protocol. (a) Due to experimental difficulties, measurements in vivo were carried out only in frogs. The experimental technique used was similar to that previously described [23]. The animal was mounted in a special holder to immobilize its legs without interfering with its respiratory movements. The sciatic nerve and femoral artery were exposed by means of a longitudinal incision on the dorsal aspect of the thigh. A 5 mm segment of artery and nerve was isolated from the underlying muscle by inserting a piece of soft teflon sheath beneath both structures. The teflon splint does not interfere with the intraneural blood microcirculation. The exposed nerve-artery segment was irrigated continuously with a Ringer's solution (101.8 mM NaCl/2.7 mM KCl/2.1 mM $MgCl_2$/1.9 mM $CaCl_2$/2.0 mM $NaHCO_3$/0.36 mM NaH_2PO_4) through three small teflon tubes at a flow rate of about 12 drops/min. The head and the thorax of the frog were located within a device connected to an anesthetic dispenser. Because of the movements of the live animals, great care had to be taken to assure that the nerves could be accurately positioned at any time during the accumulation of X-ray diffraction data of the myelin of each frog being anesthetized. This difficulty was overidden with the use of three manipulators, but nevertheless, to record high resolution X-ray patterns, we had to use isolated sciatic nerves from animals anesthetized in vivo by *n*-pentane vapors (see be-

low). The behavior of the X-ray diffraction patterns was studied during anesthesia by continuous sequential recordings of 2.5 min accumulation.(b) Experiments with isolated nerves of frogs and rats were performed in vitro. The animals were introduced inside of a jar which was connected to an anesthetic dispenser. Only animals in good conditions were used for the experimental measurements. Frogs and rats were discarded if their heart did no beat at a reasonable rate after the alkane treatment. Data were obtained from the myelin of pairs of control and experimental sciatic nerves sectioned from the same animal. The nerves were dissected in less than 2 min and mounted into a wet chamber, modified from Rud [24], which allowed to keep good physiological conditions for several hours. The control nerve was studied first. Once the irrigation was started, the nerve was supramaximally stimulated at one shot every 2.5 min during two hours. Compound action potentials were recorded, as well as the X-ray diffraction patterns of 2.5 min accumulation. While the control measurements were taking place, the live animal was exposed to *n*-pentane inhalation. At the end of the two hours treatment the experimental sciatic nerve was dissected and studied as the control.

X-ray techniques. The beam from an Elliott GX6 rotating anode X-ray generator operated at 30 kV and 30 mA was linearly focused and monochromatized by a nickel-coated bent glass mirror. Kβ radiation was attenuated by placing a Ni filter between the mirror and the specimen. Diffraction patterns were recorded by using a delay-line type position-sensitive detector, 80 mm effective length and 10 mm aperture width [25]. The nerve to detector distance was 293 mm. The techniques for sequential recording of the diffraction patterns have been described previously [21–23,26]. The patterns were stored in the magnetic tape unit of an online computer for later analysis. Plots of the computer-stored patterns were obtained using a digital plotter. The intensity of the reflections was measured from peak areas after background substraction. The period measurement from the position of the reflections was accurate to within 1%.

Electron density profiles $\rho(x)$ were calculated as previously described [26]. Different profiles were scaled by setting $\Sigma\ F^2(h)/d = \text{constant}$ [27]. Standard deviation errors $\sigma_{\rho(x)}$ in electron density profiles, were determined using classical equations of error propagation [28,29] from the corresponding standard deviation errors $\sigma_{F(h)}$ associated with each $F(h)$.

Results

Changes in 3rd and 4th order reflections during anesthesia in vivo with n-pentane

After recording an initial control pattern, frogs were exposed to *n*-pentane vapors as described in Methods and continuous sequential X-ray diffraction patterns of 2.5 min accumulation were recorded for two hours. The X-ray patterns were very similar to each other during the first hour of alkane inhalation. Then, there was a small increase in intensity of the 3rd order reflection concomitantly with a decrease of the 4th order. These type of changes kept going on very slowly for the second hour, after which the increase of the 3rd order reflection was of a 15%, whereas the 4th order intensity fell by about 30% of its original value (Fig. 1). These results, in vivo reproduced the effect previously obtained with isolated frog sciatic nerves which were perfused directly with normal Ringer solutions saturated with *n*-pentane [22].

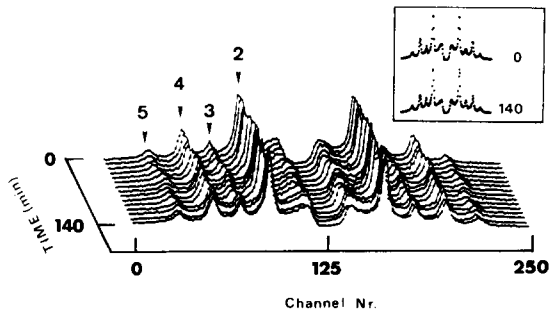

Fig. 1. Behaviour of the in vivo X-ray diffraction patterns, from the myelin of the sciatic nerve of a frog, while the animal was being anesthetized by inhalation of *n*-pentane vapors. Due to frog movements the quality of the 2.5 min accumulated counting X-ray patterns is poor at high resolution (not shown). For comparison purposes the inset shows the control (0 min) and the anesthetized (140 min) diffraction patterns. Notice the increase of the 3rd order and the decrease of the 4th order reflections with anesthesia. The position of the reflections is pointed by arrows.

Compound action potentials and simultaneous X-ray diffraction patterns on the same isolated sciatic nerve

Fig. 2 shows a series of experimental X-ray patterns obtained from an anesthetized frog sciatic nerve during the process of recovery in which it was superfused with normal Ringer solution. After 3 min of nerve dissection the following significant changes in myelin structure and electrical activity were observed in dissected anesthetized nerves as compared with freshly dissected control nerves: (1) a 60% increase in the I_3/I_4 ratio; (2) a decrease of more than 60% in the compound action potential amplitude; (3) a slowing down by about 60% of the velocity of the compound action potential. Time-courses of compound action potential amplitude (%) and ratio (I_3/I_4) of the intensities are shown in Fig. 3 for control (a) and anesthetized (b) sciatic nerve during the process of recovery by superfusion with normal Ringer solution. These parameters remained constant in the control nerve (Fig. 3a), while in the anesthetized nerve (Fig. 3b) the intensity of the 4th order reflection increased continuously and the 3rd order reflection decreased simultaneously. These two reflections attained values similar to those for the control nerve after approx 1 h of superfusion with normal Ringer solution.

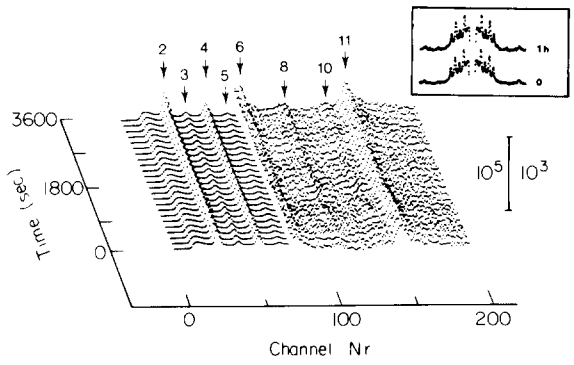

Fig. 2. Behaviour of the X-ray diffraction patterns from the myelin of the sciatic nerve of an anesthetized frog during the process of recovery by perfusion with normal Ringer solution. The three-dimensional plot shows the progressive recovery with time, of the 6th, 8th and 10th order reflections. The figure has been depicted with a different magnification for low (2 to 5) and high (6 to 11) order reflections. The scale in counts is indicated by the vertical bar and the position of the reflections is pointed by arrows. For comparison the inset shows in log scale: (0) the pattern recorded immediately after the nerve was dissected from the anesthetized animal; it can be seen that it almost lacks the 6th, 8th and 10th order reflection; (1 h) the pattern has recovered the 6th, 8th and 10th order reflections. Notice that in the recovered pattern the 3rd and 4th orders display intensities characteristic of native frog sciatic myelin.

Compound action potential recovered its normal amplitude with a more rapid kinetics than that of the structural parameter (I_3/I_4), attaining its maximum amplitude in about 30 min. The conduction velocity also started to increase at the onset of the perfusion with normal Ringer. The recovery of this parameter was closely related to the behaviour of the I_3/I_4 ratio (kinetics not shown in the figure), although similarly to compound action potential amplitude it never attained a complete recovery.

X-ray diffraction patterns from anesthetized and recovered myelin

Fig. 4 (left) shows X-ray diffraction patterns from (A) anesthetized frog sciatic nerve myelin (see Methods), and from (R) the same nerve recovered after 1 h of superfusion with normal Ringer solution. In both experimental conditions sharp reflections (12 orders) corresponding to the same lamellar repeat of about 176 Å were recorded. The reflections broaden with increasing diffraction angle [23,30–33]. In conditions of anesthesia (A), the intensities of the reflections were significantly different from the ones recorded after the recovery of the electrophysiological properties (R). In general, the odd orders were increased and the even orders were diminished in intensity for the anesthetized nerve. This is shown in Table I and in the insets of Figs. 4 (left).

A similar experiment performed with an anesthetized rat gave basically the same results obtained with frogs. Fig. 4 (right) shows X-ray patterns from (A) anesthetized rat sciatic myelin, and (R) the same nerve after recovery. In both conditions up to 12 lamellar reflections of about 178 Å repeat period were recorded. The relative intensities of the reflections were similar to those shown for frog sciatic nerves, although the magnitude of the changes between anesthetized (A) and recovered (R) myelin was slightly smaller for mammals. (Compare insets of Fig. 4).

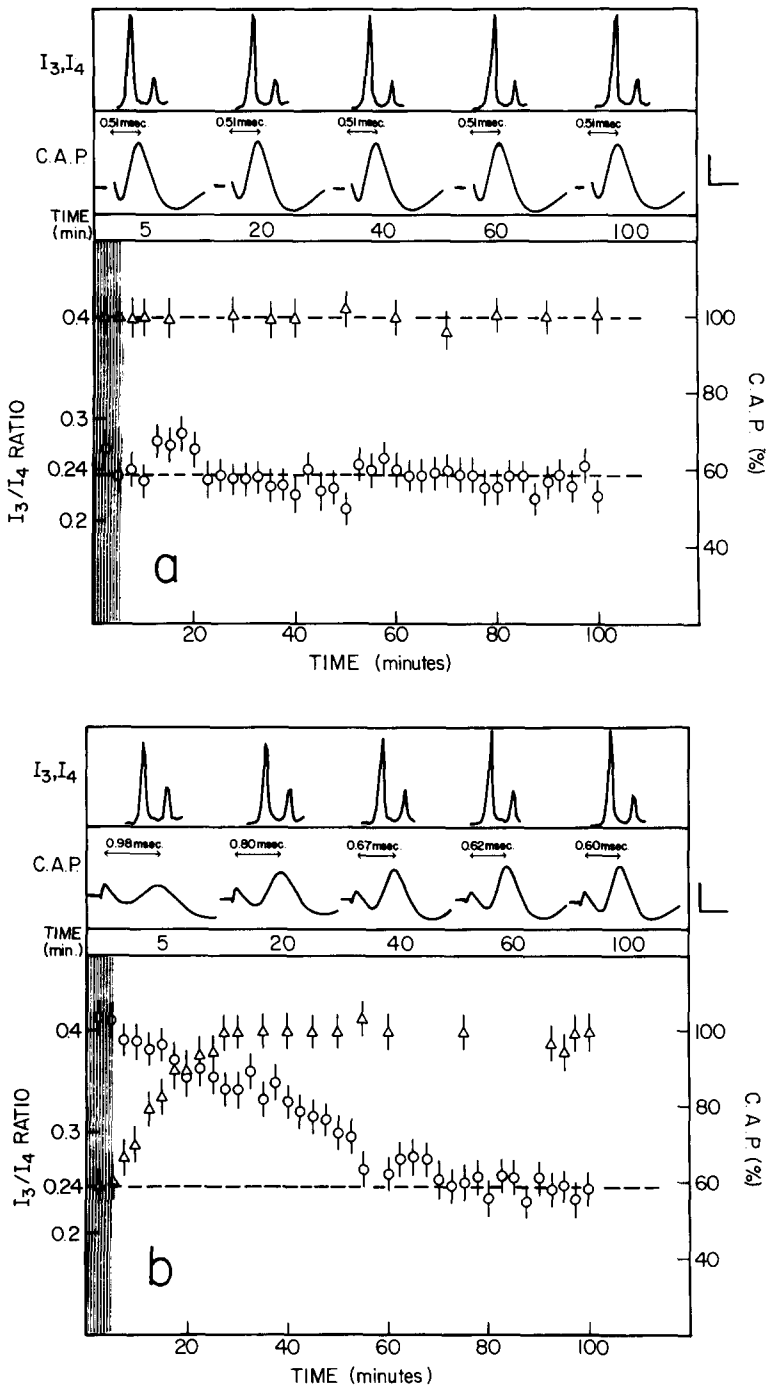

Fig. 3. Time-courses of intensities ratio (○) between the 3rd and 4th order reflections and compound action potential amplitude (C.A.P.) (Δ); (a) freshly dissected frog sciatic nerve; (b) freshly dissected sciatic nerve from an anesthetized frog. I_4, I_3 is the variation with time of the region of X-ray patterns corresponding to the 4th (higher intensity) and 3rd (lower intensity) order reflections. Underneath the patterns, records of compound action potentials obtained at different times of the kinetics can be appreciated. The calibration bars indicate: 0.25 mV (vertical) and 0.5 ms (horizontal). The standard deviation error for I_3/I_4 ratio is indicated for every measurement. The mean value (0.24) is represented by a broken line. The shaded bars indicate the 5 min time period in which the nerves were exposed to a low perfusion rate, 2 drops per min. The experiment was pursued at a rate of 20 drops per min. (a) Notice that both, compound action potential amplitude and I_3/I_4 ratio remain constant during the experiment. (b) Notice that when the rate of perfusion is increased to 20 drops per min, the compound action potential amplitude increases attaining its maximum value (100%) in some 30 min (see also the experimental records at the upper part). On the contrary, the I_3/I_4 ratio attained the value for the control nerve (0.24, broken line) in about 60 min. The I_4,I_3 patterns show the increase in intensity of the 4th order and the simultaneous decrease of the 3rd order reflection. Notice also that the recovery of conduction velocity, indicated by the elapsed time between the stimulus artifact and compound action potential maximum, follows a slower kinetic than that of compound action potential.

Electron density profiles of anesthetized and recovered myelin

Fig. 5a shows the electron density profiles and associated errors determined for anesthetized and recovered frog sciatic nerve myelin using the data of Table I. Despite the apparently large differences between the corresponding patterns of Fig. 4, the calculated electron density distributions

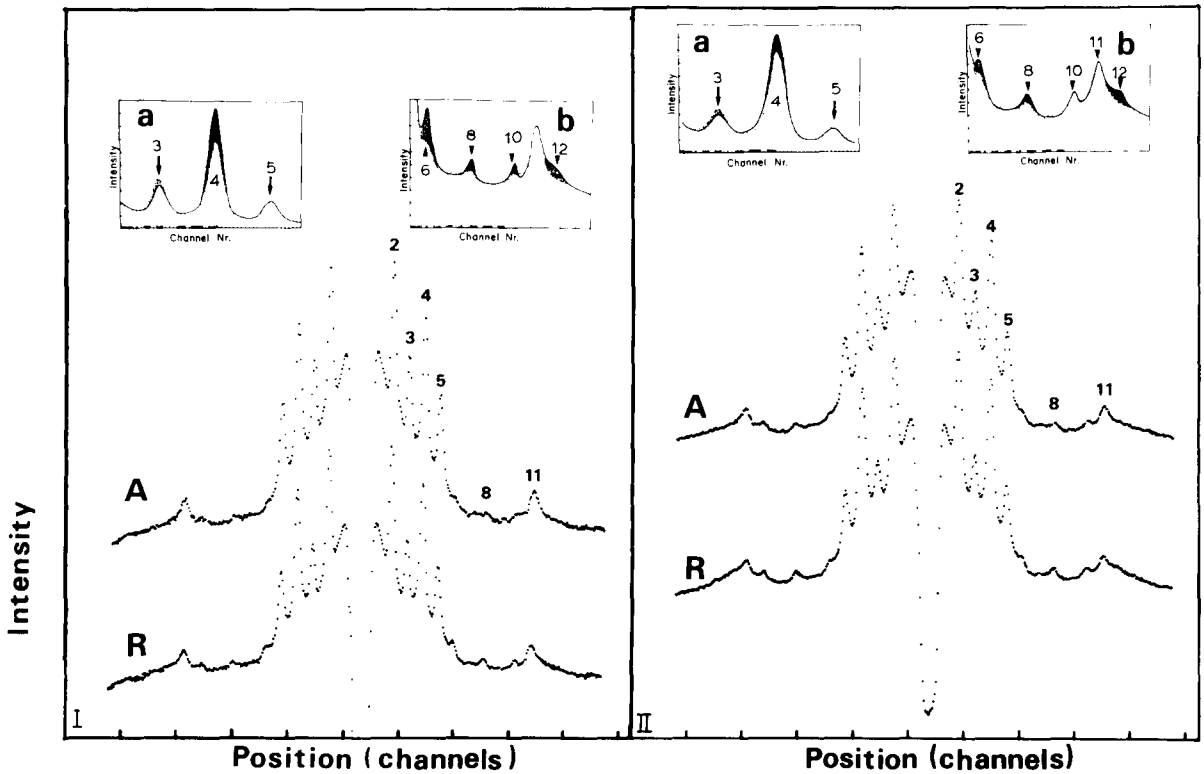

Fig. 4. Logarithmic plots of X-ray diffraction patterns recorded during 15 min from the sciatic nerve myelin from a frog (left, I) and a rat (right, II). A, nerve isolated from the animal anesthetized by *n*-pentane inhalation. R, the same nerve recovered after 1 h of perfusion with normal Ringer solution. In both conditions the myelin lattice thickness was identical. (176 Å for the frog nerve; 178 Å for the rat nerve). Linear plots of superimposed patterns of myelin from anesthetized and recovered nerve are shown in the insets for the low (a) and high (b) order reflections. Shaded regions indicate the excess intensity of the recovered pattern as compared with the anesthetized pattern. The 3rd order shows a different type of shadowing since the excess intensity has an opposite sense. Notice that the excess intensity of the even reflections, apparent in the insets, is larger in frogs than in mammals.

TABLE I

COMPARISON OF X-RAY DIFFRACTION PARAMETERS BETWEEN ANESTHETIZED AND RECOVERED FROG SCIATIC MYELIN

	Anesthetized					Recovered					
h	$I_t(h)$	$B(h)$	$I(h)$	$F_A(h)$	$\sigma_{F_A(h)}$	$I_t(h)$	$B(h)$	$I(h)$	$F_R(h)$	$\sigma_{F_R(h)}$	$\Delta F(h)\%$
+2	450319	150727	299592	774	1.42	518844	172596	346248	832	1.41	+7.5
+3	142711	77445	65266	442	2.76	130498	80253	50245	388	3.07	−12.2
−4	235710	76530	159180	798	2.80	309056	97302	211754	920	2.77	+15.3
−5	93612	51667	41944	458	4.65	89317	50605	38712	440	4.75	−3.9
+6	20676	19822	875	72	20.65	24203	21645	2558	124	12.70	+72.2
7	12195	12195	0	0	28.41	18373	18373	0	0	29.37	0
+8	14775	13392	721	76	18.05	22292	19727	2564	143	16.19	+88.2
9	10455	10455	0	0	45.28	15068	15068	0	0	42.19	0
+10	14335	14019	403	64	47.40	15371	14013	1358	117	23.26	+82.8
+11	23564	16188	7376	285	12.77	25024	18315	6709	272	13.98	−4.56
−12	7528	6662	865	102	24.30	20933	18304	2629	178	23.18	+74.5

h, diffraction order; $I_t(h)$, integral of total counts for each reflection; $B(h)$, integrated intensity of the background scattering under each reflection; $I(h) = I_t(h) - B(h)$; $F(h)$ and $\sigma_{F(h)}$ are the calculated structure factors and the corresponding standard deviation errors. $\Delta F(h)\% = [(F_A(h) - F_R(h))/F_A(h)] \times 100$. The subscripts A and R indicate anesthetized and recovered, respectively. The phase combination used to calculate the electron density profiles of Fig. 5 is indicated. Data are related to the experimental patterns of Fig. 4I.

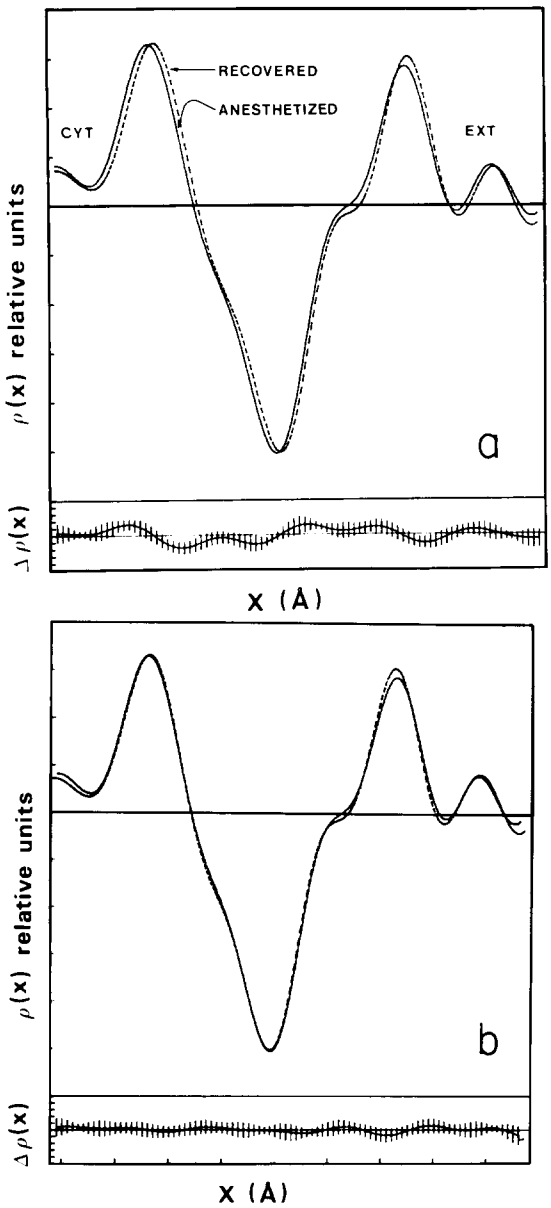

Fig. 5. (a) Electron density profiles of a single myelin membrane from anesthetized (continuous line) and recovered (dotted line) frog sciatic nerve. The profiles have been calculated using the data of Table I which correspond to diffraction patterns of Fig. 4 (left, I). The electron densities are represented in the ordinate in relative units. The difference $\Delta\rho(x)$ between anesthetized and recovered profile is shown at the same scale at the bottom of the figure. The short vertical bars, spaced 1 Å apart, represent ± 1.645 standard deviations (90% confidence level). As compared to the recovered myelin (dotted profile) the anesthetized membrane (continuous profile) is shifted towards the cytoplasmic side. (b) The recovered dotted profile has been shifted towards the cytoplasmic side by 0.8 Å. Notice that the two profiles are practically identical.

are very similar. However, the differences profiles $\Delta\rho(x)$, shown at the bottom of the figure, which was calculated substracting the continuous anesthetized profile from the dotted profile for recovered myelin, indicates that the magnitude and location of electron density changes are statistically significant at a 90% confidence level. From the first glance it is obvious, that the main difference between the two profiles of Fig. 5a, lies in the relative position of the membrane within the myelin unit cell. In fact the two myelin profiles show almost a perfect structural coincidence when one is shifted 0.8 Å relative to the other as shown by the differences profiles $\Delta\rho(x)$ at the bottom of Fig. 5b.

Discussion

In order to determine the changes in myelin structure occurring during the process of anesthesia by *n*-pentane, we recorded accurate X-ray diffraction patterns from anesthetized sciatic nerve myelin at the highest possible resolution. Fig. 4 display high quality patterns showing lamellar reflections up to a resolution of about 15 Å. The patterns corresponding to anesthetized (A) frog (left) and rat (right), show changes in the intensity of the 3rd and 4th order reflections similar to the ones observed in earlier experiments [22]. Therefore, the results obtained at high resolution from animals anesthetized in vivo by inhalation of *n*-pentane vapors and recorded either, directly in vivo or isolated after anesthesia are equivalent to those obtained at low resolution from sciatic nerves perfused with Ringer solutions saturated with *n*-pentane [21,22].

Kinetical measurements of changes in X-ray patterns and compound action potentials

The structural measurements carried out on sciatic nerve myelin in vivo while the frog is being anesthetized opens the possibility to work on the molecular effects of drugs or agents in myelin membranes, in whole live animals. Our results show that the effect of *n*-pentane on myelin structure in the in vivo experiment is more rapid that the previously observed when the nerve was dissected and perfused with an alkane saturated solution [21,22].

The use of nerves isolated from anesthetized animals has allowed us to investigate the kinetic relationships between physiological parameters (compound action potential amplitude and velocity of nerve impulse propagation) and structural changes occurring in a natural membrane system such as the myelin sheath, which is intimately associated to the axolema membrane. When the anesthetized nerve was superfused extensively with normal Ringer solution, compound action potential recovered its maximum amplitude in about 30 min (Fig. 3b), contrarily to what happened with the structural recovery process, which took more than 1 h. This is not a suprising result as compound action potential is generated at the Ranvier node which is more exposed to the external space, thus allowing a faster turnover of fluids and ions that in myelin.

The fact that the compound action potential amplitude is almost completely recovered when the myelin is still structurally altered, indicates that the process of impulse generation at the node of Ranvier is poorly related to the internodal myelin structure [34]. However, Fig. 3b shows that structure and conduction velocity follow similar kinetics, which suggests some coupling between these processes. This physiological relationship will be investigated more deeply in further studies.

Myelin membrane structure from anesthetized and recovered sciatic nerves

X-ray patterns from anesthetized and recovered sciatic nerve myelin, show a similar broadening of the reflections with increasing diffraction angle (compare patterns A and R in Fig. 4), indicating that *n*-pentane does not perturbs significantly the lattice. This is consistent with a neutron and X-ray diffraction study carried out on oriented multilamellar lipid-water systems [35], which demonstrated that clinical concentrations of various general anesthetics do not change the structure of lipid bilayers and that an increase of 10–20-times those concentrations produces a blurring of the high-angle reflections with the consequent loss of resolution in the electron density profiles. Also in agreement with the results of model lipid-water systems, Fig. 5 indicates that, at 15 Å resolution, myelin membrane bilayer structure remains almost unchanged during *n*-pentane anesthesia. This last result is not in accordance with the thickness-tension hypothesis [18] which establishes that membrane bilayer thickness increases significantly during anesthesia. In order to obtain direct definite proofs on this matter, similar experiments to those carried out on myelin have to be performed on axolema membranes using some more conventional anesthetics.

The electron density profiles from myelin of anesthetized and recovered nerve (Fig. 5) indicate that the membrane structure is very similar in both circumstances. The main difference consists in a variation of the relative position of membrane units within the lattice, which in anesthetized myelin are more closely packed towards the cytoplasmic side. The profiles of Fig. 5 show that the decrease by about 1.6 Å in the cytoplasmic space is accompanied by about 1 Å increased separation of the external space. This suggests that most likely *n*-pentane changes the surface interactions between adjacent membrane pairs which must then attain a new equilibrium position [36]. The different responses to anesthesia by *n*-pentane at the cytoplasmic and external surfaces confirm that the chemical composition of these membrane surfaces is distinct [37,38] and consequently they show different intermembrane interactions.

The change in surface interactions between adjacent nerve myelin membranes from animals anesthetized in vivo is not observed in lamellar phases of pure lipid-water systems [35]. We note, however, that these experiments were done with uncharged lipids. Therefore, our conclusion is that the observed surface effect may be related to charged components, either or both, lipids and proteins. The notion that membrane proteins might be important in anesthesia has been stated by other groups [35,39,40].

Possible relationship between anesthesia by n-pentane and myelin structural changes

The results reported in the present work, although not directly related to the excitable membranes, may be useful to gain further insight in the process of anesthesia and should be considered within the context of the following observations. First, the antagonistic action of high pressures against anesthesia indicates a positive excess volume of the system when anesthetics are in-

corporated [6–10]. Eyring et al. [13] proposed that anesthetic molecules interact with hydrophobic regions of membrane proteins essential in maintaining nervous activity, thereby causing a conformational change to a less active state, with formation of salt bridges in proteins and consequent charge neutralization and volume expansion [13]. Second, the current concept dealing with myelin stability states [41–45] that myelin membrane lattice is maintained by a balance of forces: Van der Waal's attractive forces tending to decrease membrane separation and electrostatic repulsive forces tending to increase membrane separation. The equilibrium of these physical forces determines lattice dimensions and positions of the membranes within the unit cell. Besides, it has been proposed (see Ref. 49 for review) that a rigid spacer protein molecule projects from the bilayer into the extracellular space. In peripheral myelin the projecting molecule has been suggested to be the Po protein, which is the major protein of sciatic nerve myelin [38,47]. This molecule would determine the minimum thickness of the external space in native physiological conditions.

The thinning of the cytoplasmic space that we have observed concomitantly with the process of anesthesia by *n*-pentane in vivo can be attributed to decreased electrostatic repulsion between internal membrane surfaces [48]. This interpretation is supported by experiments carried out in other laboratories which showed that anesthetics increase cation binding to membranes [49,50]. At present, we do not know what causes the accompanying smaller increase in separation at the external boundary.

Since our results have been interpreted in terms of charge neutralization in myelin membranes, during anesthesia, it should be possible that a similar phenomenon could take place at the excitable axolema membranes where it has been demonstrated [51–53] that surface charge density is crucial for the excitability of ionic channels.

Acknowledgements

The authors wish to thank Dr. A. Gabriel (E.M.B.L., Grenoble Outstation) for the continuous support with the position sensitive detectors, Dr. R. Padrón for discussions, suggestions and experimental help at the very beginning of this work; Drs. G. Whittembury and E. Vonasek for the careful and critical reading of the manuscript. O. Morán was supported by the Vollmer Foundation to attend the Ph.Sc. program at Centro de Estudios Avanzados, IVIC (Venezuela). This work was supported in part by a project (S1-1413) from CONICIT (Venezuela) granted to L. Mateu.

References

1 Mullins, L.J. (1975) in Molecular Mechanism of Anesthesia, Progress in Anesthesiology, Vol. 1 (Fink, R., ed.), pp. 237–242
2 Seeman, P. (1975) in Molecular Mechanisms of Anesthesia, Progress in Anesthesiology, Vol. 1 (Fink, R., ed.), pp. 243–251
3 Trudel, J.R. and Cohen, E.N. (1975) in Molecular Mechanisms of Anesthesia, Progress in Anesthesiology, Vol. 1. (Fink, R., ed.), pp. 315–321
4 Singer, S.J. and Nicholson, G.L. (1972) Science 175, 720–730
5 Graham, D.E. and Lea, E.A.J. (1972) Biochim. Biophys. Acta 274, 286–293
6 Bogs, J.M., Yoong, T. and Hsia, J.C. (1976) Mol. Pharmacol. 12, 127–135
7 Johnson, S.M. and Miller, K.W. (1970) Nature (London) 288, 75–76
8 Chin, J.H., Trudell, J.R. and Cohen, E.N. (1976) Life Sci. 18, 489–498
9 Halsey, M.J. and Wardely-Smith, B. (1975) Nature (London) 257, 811–813
10 Miller, K.W. and Wilson, M. (1979) Anesthesiology 48, 104–110
11 Nemethy, G. and Scheraga, H.A. (1962) Anal. Chem. Phys. 36, 3382–3400
12 Lumry, R. and Biltonen, R. (1969) in Structure and Stability of Biological Macromolecules, Vol. 2 (Timasheff, S.N. and Fasman, G.D., eds.), pp. 65–114, Marcel Decker, New York
13 Eyring, H., Woodbury, J.W. and D'Arrigo, J.S. (1973) Anesthesiology 38, 415–424
14 Ueda, I., Kamaya, H. and Eyring, H. (1976) Proc. Natl. Acad. Sci. USA 73, 481–485
15 Okuda, C. (1982) J. Biochem. 92, 357–363
16 Drost-Hansen, W. (1971) in Chemistry of the Cell Interface, Part B (Brown, H.D., ed.), pp. 1–165, Academic Press, New York
17 Tait, M.N. and Franks, F. (1971) Nature 230, 91–94
18 Haydon, D.A., Hendry, B.M., Levinson, S.R. and Requena, J. (1977) Nature 268, 356–358
19 Huxley, A.F. and Stämpfli, R. (1948) J. Physiol. 108, 315–339
20 Stämpfli, R. (1954) Physiol. Rev. 34, 101–112
21 Padrón, R., Mateu, L. and Requena, J. (1979) Biochim. Biophys. Acta 552, 535–539

22 Padrón, R., Mateu, L. and Requena, J. (1980) Biochim. Biophys. Acta 602, 221–233
23 Padrón, R. and Mateu, L. (1981) J. Neurosci. Res. 6, 251–260
24 Rud, J. (1961) Acta Physiol. Scand. 51, 17–25
25 Gabriel, A. (1979) Rev. Sci. Instrum. 48, 1303–1305
26 Padrón, R. and Mateu, L. (198) J. Neurosci. Res. 5, 611–620
27 Blaurock, A.E. (1971) J. Mol. Biol. 56, 35–52
28 Topping, J. (1972) Errors of Observation and Their Treatment, John Wiley & Sons, New York
29 Kirschner, D.A. and Sidman, R.L. (1976) Biochim. Biophys. Acta 448, 73–87
30 Worthington, C.R. and McIntosh, T.J. (1973) Nature New Biol. 245, 97–99
31 Worthington, C.R. and McIntosh, T.J. (1974) Biophys. J. 14, 703–729
32 Blaurock, A.E. and Nelander, J.C. (1976) J. Mol. Biol. 103, 421–431
33 Nelander, J.C. and Blaurock, A.E. (1978) J. Mol. Biol. 118, 497–532
34 Bostock, H. and Sears, T.A. (1978) J. Physiol. 280, 273–301
35 Franks, N.P. and Lieb, W.R. (1979) J. Mol. Biol. 133, 469–500
36 Rand, R.P., Fuller, N.L. and Lis, J.L. (1979) Nature 279, 258–260
37 Caspar, D.L.D. and Kirschner, D.A. (1971) Nature New Biol. 231, 46–52
38 Golds, E.E. and Braun, P.E. (1976) J. Biol. Chem. 251, 4729–4734
39 Franks, N.P. and Lieb, W.R. (1978) Nature 274, 339–342
40 Richard, C.C., Martin, K., Gregory, S. Keightley, C.A. Hesketh, T.E., Smith, C.A., Warren, G.B. and Metcalf, J.C. (1978) Nature 276, 775–779
41 Finean, J.B. and Millington, P.F. (1957) J. Biophys. Biochem. Cytol. 3, 89–94
42 Worthington, C.R. and Blaurock, A.E. (1969) Biochim. Biophys. Acta 173, 427–435
43 Padrón, R., Mateu, L. and Kirschner, D.A. (1979) Biophys. J. 28, 231–239
44 Padrón, R. and Mateu, L. (1982) Biophys. J. 39, 183–188
45 Morán, O. and Mateu, L. (1983) Nature 304, 344–345
46 Blaurock, A.E. (1982) Biochim. Biophys. Acta 650, 167–207
47 Peterson, R.G. and Gruener, R.W. (1978) Brain Res. 152, 17–29
48 Worcester, D. (1983) Proceedings of the Advanced Course on Anesthesia: Basic Mechanisms in Cellular Membranes (CLAB-UNESCO-IVIC), Caracas, Venezuela
49 Seeman, P., Chau, H., Goldberg, M. Sauks, T. and Sax, L. (1971) Biochim. Biophys. Acta 225, 185–193
50 Seeman, P. (1972) Pharmac. Rev. 24, 583–655
51 Frankenhauser, B. (1957) J. Physiol. 137, 245–260
52 Frankenhauser, B. and Hodgkin, A.L. (1957) J. Physiol. 137, 218–244
53 Fernández, J.M., Bezanilla, F. and Taylor, R.E. (1982) Nature, 297, 150–152